Aceruloplasminemia

Retinal Histopathologic Manifestations and Iron-Mediated Melanosome Degradation

Natalie Wolkow, PhD; Ying Song, MD; Ting-Di Wu, PhD; Jiang Qian, MD, PhD; Jean-Luc Guerquin-Kern, PhD; Joshua L. Dunaief, MD, PhD

Objective: To examine the retinal histopathologic manifestation of aceruloplasminemia, an autosomal recessive disease caused by mutation of the ferroxidase ceruloplasmin, resulting in tissue iron overload.

Methods: The morphologic features of the human aceruloplasminemic retina were studied with light and electron microscopy. Retinal iron accumulation was assessed with Perls Prussian blue staining, immunohistochemistry, and secondary ion mass spectrometry.

Results: Light and electron microscopic analysis revealed several ocular pathologic findings that resembled age-related macular degeneration, including retinal pigment epithelium (RPE) depigmentation, atrophy and hypertrophy, nodular and diffuse drusen, and lipofuscin and melanolipofuscin granules. Complement deposition was detected in drusen. The RPE cells and neural retina had increased levels of iron. Two major types of RPE cells were observed: melanosome rich and melanosome poor. Melanosome-rich cells had increased levels of iron and melanolipofuscin. The melanolipofuscin granules were observed in large aggregates, where some of the melanosomes were degrading. Melanosome-poor cells lacked melanosomes, melanolipofuscin, and lipofuscin but contained electron-dense aggregates high in iron, phosphorus, and sulfur.

Conclusions: The findings in the aceruloplasminemic retina resemble some of those found in age-related macular degeneration. Also, they suggest that melanosomes in the RPE can be degraded via iron-mediated reactive oxygen species production.

Clinical Relevance: Mechanisms underlying the pathologic mechanisms found in aceruloplasminemia also may be important in age-related macular degeneration.

Arch Ophthalmol. 2011;129(11):1466-1474

Author Affiliations: F. M. Kirby Center for Molecular Ophthalmology, Scheie Eye Institute, Perelman School of Medicine, University of Pennsylvania, Philadelphia (Drs Wolkow and Song and Dunaief); Institut Curie, Laboratoire de Microscopie Ionique (Drs Wu and Guerquin-Kern) and Institut National de la Santé et de la Recherche Médicale (Drs Wu and Guerquin-Kern), Orsay, France; and Department of Pathology and Laboratory Medicine/Affiliated Pathology Services, Inc, Albany Medical College and Center, Albany, New York (Dr Qian).

ACERULOPLASMINEMIA IS A rare autosomal recessive disease[1] caused by mutation of the ceruloplasmin gene.[2] Aceruloplasminemia is characterized by a triad of diabetes mellitus, retinal degeneration, and neurodegeneration that usually manifests between the ages of 30 and 55 years.[3-5] The disease is caused by iron accumulation in the pancreas, liver, brain, and retina due to a decrease in iron export.[4-6]

Ceruloplasmin is a ferroxidase protein that is secreted from cells or is glycosylphosphatidylinositol linked to the outer surface of cell membranes.[7] Ceruloplasmin interacts with ferroportin, the cellular iron exporter, to export ferrous iron from cells.[8] As a ferroxidase, ceruloplasmin converts ferrous to ferric iron, allowing ferric iron to bind to transferrin in the plasma.[8] Lack of ceruloplasmin, even in the presence of ferroportin, markedly impairs iron export from cells.[9] Thus, ferroxidases are necessary components for iron export.

In retinas with age-related macular degeneration (AMD), iron and transferrin levels are elevated, suggesting that iron toxicity may contribute to the pathogenesis of AMD.[10,11] Furthermore, in mice, combined knockout of ceruloplasmin and mutation of its homologue, hephaestin, causes retinal and brain iron accumulation and degeneration.[12,13] This retinal degeneration resembles AMD.[13]

Pathologic studies[3-5] of many aceruloplasminemic tissues have been published; however, no study has examined retinal histopathologic manifestations, to our knowledge. The only published reports focusing on the retina have been clinical case reports, which have shown pigmentary abnormalities in the peripheral retina.[14,15] In 2005, one of us[15] published a clinical re-

©2011 American Medical Association. All rights reserved.
Downloaded From: https://jamanetwork.com/ on 03/04/2022

port of an individual with aceruloplasminemia. In the present study, we examine the retinal histopathologic features of the same individual at age 60 years.

METHODS

TISSUE PREPARATION

Eyes were obtained from a 60-year-old male donor with aceruloplasminemia after a 7-hour postmortem interval, in accordance with the tenets of the Declaration of Helsinki. At the time of the previous study,[15] the donor had iron deficiency anemia, long-standing diabetes mellitus, cardiomyopathy, iron accumulation in the liver, dementia, and macular degeneration characterized by drusen and areas of retinal pigment epithelium (RPE) depigmentation.[15] Subsequent to the publication of the report, he had experienced many hypoglycemic episodes, had developed renal failure, had been hospitalized, had developed aspiration pneumonia and sepsis, and had died. For the present study, samples from the anterior segment; retina, choroid, and sclera; and optic nerve of his right eye were used. As a normal control, an eye from a 60-year-old male donor with a 7-hour postmortem interval and no history of retinal disease was obtained from the Lions Eye Bank. A control eye with AMD was obtained from an 86-year-old woman with a history of AMD after a postmortem interval of 20 hours from the Complications of Age-Related Macular Degeneration Prevention Trial Eye Donor Program in collaboration with the Foundation Fighting Blindness. All eyes were fixed in formalin, embedded in paraffin, and sectioned at 7-μm thickness.

PERIODIC ACID–SCHIFF STAINING

Paraffin sections from the ocular regions indicated herein were stained using a periodic acid–Schiff stain kit (Polysciences, Inc, Warrington, Pennsylvania) as suggested by the manufacturer. Images were acquired on a Nikon Eclipse TE300 camera (Nikon Corporation, Tokyo, Japan) using Image-Pro Plus software, version 6.1 (Media Cybernetics, Inc, Bethesda, Maryland). Histopathologic analysis was performed as previously described.[16]

PERLS PRUSSIAN BLUE STAINING FOR IRON

Paraffin sections were bleached with 0.25% potassium permanganate and 0.50% oxalic acid. Then, they were stained with 5% potassium ferrocyanide and 5% hydrochloride for 30 minutes.

IMMUNOHISTOCHEMISTRY

Paraffin sections were stained using the Vectastain ABC Alkaline Phosphatase for Rabbit and Mouse IgG and Vector BCIP-NBT kits (Vector Laboratories, Inc, Burlingame, California). Primary antibodies for L-ferritin (F-17; gift of Paolo Arosio, PhD, and Paolo Santambrogio, PhD), C5b-9 (M0777; Dako, Carpinteria, California), and vitronectin (MAB1945; Millipore, Billerica, Massachusetts) were used at 1:100 dilutions.

ELECTRON MICROSCOPY

The temporal macula was postfixed with osmium tetroxide, dehydrated, and embedded in EMbed-812 (Electron Microscopy Sciences, Hatfield, Pennsylvania). Thin sections were stained and examined with a JEOL1010 transmission electron microscope (JEOL Ltd, Tokyo, Japan). Images were acquired with Advanced Microscopy Techniques Image Capture software (Advanced Microscopy Techniques, Corp, Woburn, Massachusetts) and were rotated and cropped with Adobe Photoshop (Adobe Systems Incorporated, San Jose, California).

QUANTIFICATION OF MELANOSOMES, LYSOSOMES, AND COMPLEX GRANULES

Images of 16 consecutive melanosome-poor and 16 melanosome-rich RPE cells were taken (original magnification ×10 000) on a previously unexamined section. The RPE granules were quantified as previously described.[17]

SECONDARY ION MASS SPECTROMETRY

Secondary ion mass spectrometry (SIMS) is used to analyze the spatial distribution of elements in a sample at a resolution as high as 50 nm.[18] Samples for SIMS analysis were prepared as for transmission electron microscopy but with modifications; samples were not postfixed in osmium tetroxide, and sections were not stained with uranyl acetate or lead citrate. Thin (40-nm) and thick (150-nm) sections were cut and imaged with a JEOL1010 transmission electron microscope and then analyzed with a NanoSIMS 50 ion microprobe (CAMECA SAS, Gennevilliers, France) operating in scanning mode.

RESULTS

To determine whether the aceruloplasminemic eye had any unique pathologic manifestations, it was examined at the gross, light microscopic, and electron microscopic levels. At the gross level, the phakic right eye had no abnormalities other than macular degeneration, consistent with the results of the previous clinical report.[15]

At the light microscopic level, the cornea, iris, ciliary body, and optic nerve had normal morphologic findings (data not shown). The peripheral and macular neural retina had normal findings (**Figure 1** A and B), but the RPE cells and Bruch's membrane contained many pathologic manifestations on all sections examined, similar to those previously described in AMD.[16] Nodular drusen[16,19-21] were present in the macular, although they were much more common in the periphery (Figure 1C). The periphery also had many diffuse drusen[16,19,20] (Figure 1D), but the macula had none. The macula had subretinal drusenoid deposits[22,23] (Figure 1E); the periphery did not. The macula and periphery had RPE cells with inclusions[16,21] (Figure 1F) and RPE cells that had extruded from their normal layer[16,24] (Figure 1G). The macula had several areas of RPE hypertrophy[16] (Figure 1H) and atrophy[16] (Figure 1I); the periphery did not. The macula and the periphery had areas of depigmented RPE cells that lacked the brown color of their neighbors and instead stained purple (Figure 1J and K); normal control and AMD RPE cells lacked this color variation (Figure 1L and M).

At the electron microscopic level, drusen and basal linear deposits resembled deposits previously described in AMD[16,25-27] (**Figure** 2A-E). Also, similar to AMD, aceruloplasminemic drusen had evidence of complement activation[28-31] (**Figure** 3A-D).

To determine whether iron had accumulated in any cells, the Perls stain was performed. Strong staining was seen in the RPE of the periphery and the macula (**Figure 4**B, D, F, H, and J), but the periphery did not have as many Perls-positive cells. Hypertrophic RPE cells

©2011 American Medical Association. All rights reserved.
Downloaded From: https://jamanetwork.com/ on 03/04/2022

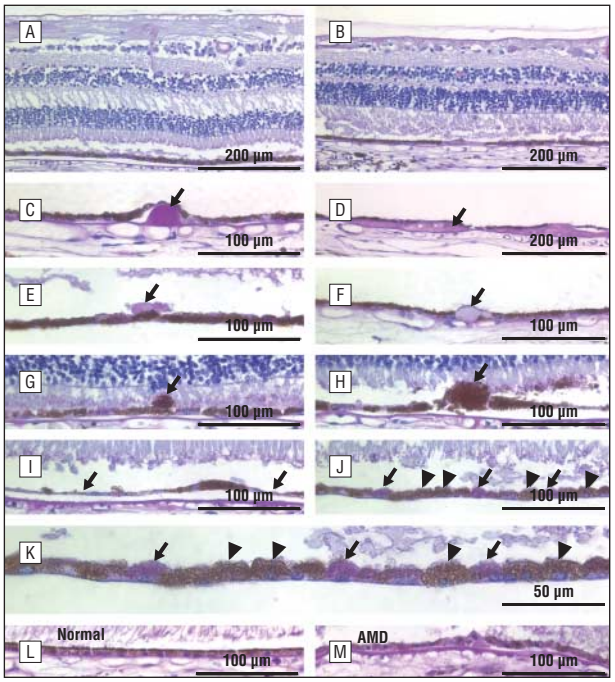

Figure 1. Paraffin-embedded sections of peripheral and macular retina stained with periodic acid–Schiff and hematoxylin. For parts A and B, original magnification ×20; parts C-J, original magnification ×40; part K, image acquired at original magnification ×40 but enlarged to ×80 by computer; parts L and M, original magnification ×40. A, Macula. B, Periphery. C, Nodular drusen (arrow) from the periphery. D, A diffuse druse (arrow) from the periphery. E, Subretinal drusenoid deposits (arrow) from the macula. F, Retinal pigment epithelium (RPE) inclusions (arrow) from the periphery. G, An extruded RPE cell (arrow) from the macula. H, A hypertrophic RPE cell (arrow) from the macula. I, Thinning and atrophy of the RPE (arrows) in the macula. J, Areas of pigmented (arrowheads) and depigmented (arrows) RPE cells. K, Image in part J enlarged. L, RPE cells from normal control eye; and M, RPE cells from the control eye with age-related macular degeneration (AMD).

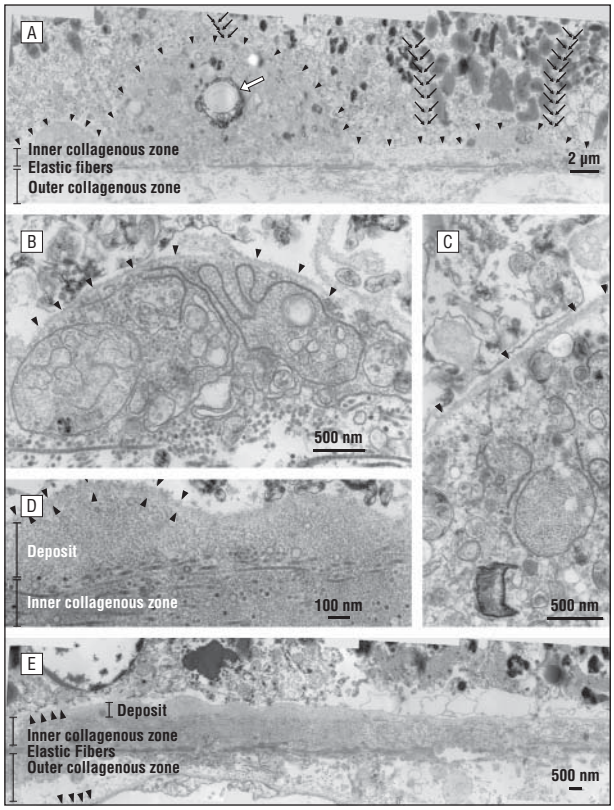

Figure 2. A druse and a basal linear deposit (composites of images). A, A druse flanked by 2 deposits (original magnification ×10 000). The retinal pigment epithelium (RPE) basal lamina is demarcated by arrowheads. These deposits contain membranous components and a crystallized area (white arrow). Melanosome-rich and melanosome-poor RPE cells sit on top of the deposits; cell boundaries are marked by black arrows. B and C, Enlarged images of the deposits in part A (for each, original magnification ×50 000). D, Enlarged image of part E; basal linear deposit containing homogeneously granular material (original magnification ×100 000). Arrowheads indicate RPE basal lamina. E, Basal linear deposit (original magnification ×20 000). RPE and choroidal basal laminae are marked by arrowheads.

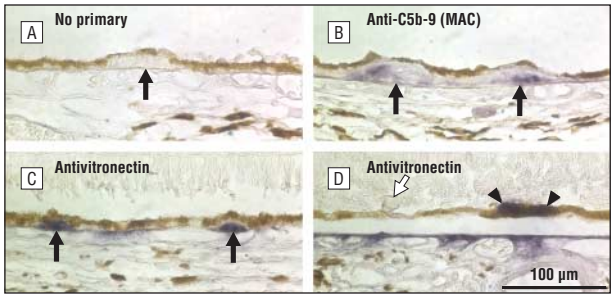

Figure 3. Drusen immunostained for C5b-9 and vitronectin (original magnification ×40). A, No primary antibody. Arrow indicates a druse. B, Anti-C5b-9 MAC (membrane attack complex) staining of drusen (arrows). C, Antivitronectin staining of drusen (arrows). D, Antivitronectin staining of retinal pigment epithelium (arrowheads) but no staining of a subretinal drusenoid deposit (white arrow).

were always Perls positive (Figure 4J). The neural retina, choroid, optic nerve, ciliary body, iris, trabecular meshwork, and cornea were Perls negative (data not shown). Of interest, many RPE cells that subsequently had a strong Perls-positive label could never be fully bleached but retained a golden color, presumably from the high iron accumulation (Figure 4E-J).

To determine whether the neural retina and Perls-negative RPE cells had increased iron levels compared with control cells, immunohistochemistry for the iron storage protein L-ferritin was performed. The neural retina (**Figure 5**F) and peripheral and macular RPE cells had strong L-ferritin staining, more than that of the normal control retina (Figure 5G-N). In control and aceruloplasminemic RPE cells, the macula had stronger L-ferritin staining than the periphery (Figure 5G-N). Although the aceruloplasminemic macula had a strong L-ferritin label, the golden cells with large iron deposits did not stain strongly with L-ferritin, suggesting that iron in them may not be stored as ferritin (Figure 5L and N).

To determine whether increased iron levels affected the normal RPE cytoarchitecture, cells were examined by electron microscopy. The aceruloplasminemic RPE mitochondria had abnormal electron-dense inclusions (**Figure 6**C and F). Normal RPE cells lacked these inclusions (Figure 6A and D), but RPE cells with AMD had occasional inclusions (Figure 6B and E). Such inclusions have not been previously described in RPE mitochondria, to our knowledge. Analysis via SIMS detected no increase in iron in the inclusions above the background tissue level, suggesting that the inclusions are areas of damaged lipids or proteins and not areas of significant iron deposits (data not shown).

©2011 American Medical Association. All rights reserved.
Downloaded From: https://jamanetwork.com/ on 03/04/2022

Electron microscopic examination of unstained sections revealed 2 major types of RPE cells: melanosome-poor cells that had many electron-dense particles (**Figure 7**A, arrows) and melanosome-rich cells that lacked the electron-dense particles (Figure 7A, arrowheads). Such particles were never seen in eyes with AMD and normal control eyes (data not shown) and have not been previously reported, to our knowledge. Stained sections revealed melanosome-rich, melanosome-poor, and a few intermediate cells, suggesting a possible progression from the melanosome-rich to the melanosome-poor phenotype over time (Figure 7B-D).

In addition to melanosomes, the melanosome-rich cells contained lipofuscin and complex granules; all these structures are seen in AMD and with aging (Figure 7E).[17,32] For 16 melanosome-rich RPE cells, the mean (SD) numbers of melanosomes, lipofuscin, and complex granules per cellular cross-section were 20.0 (7.8), 35.0 (12.0), and 11.0 (6.1), respectively.

In the melanosome-rich cells, a progression from a normal amount of melanosomes to large aggregates of melanosomes in lipofuscinoid material was observed (Figure 7F-L). The melanosomes in these aggregates could be intact (Figure 7J) or in different states of degradation (Figure 7K and L). Intermediate cells contained many more aggregates of degrading melanosomes than the melanosome-rich cells. In most cases, intact melanosomes no longer could be distinguished (Figure 7M). Aggregates with degrading melanosomes were not observed in normal control eyes or in control eyes with AMD (data not shown).

Melanosome-poor RPE cells lacked melanosomes, lipofuscin, and complex granules. For 16 melanosome-poor RPE cells, the mean (SD) number of melanosomes, lipofuscin, and complex granules per cell profile were 1.8 (2.8), 1.0 (1.5), and 0.8 (1.4), respectively. Melanosomes and complex granules were never seen outside the RPE in the pre-RPE or sub-RPE spaces, suggesting that melanosomes had not been extruded but had been degraded. Melanosome-poor RPE cells had many electron-dense, irregularly shaped membrane-bound granules that resembled siderosomes[33,34] (Figure 7N-P). Such granules were never seen in normal RPE cells or RPE cells with AMD (data not shown) and have not been previously described in the RPE, to our knowledge.[17,27,32]

To determine the subcellular location of iron in the RPE, unstained sections were examined by electron microscopy and SIMS. Complex granules from melanosome-rich aceruloplasminemic RPE cells had thin, grainy electron-dense borders (**Figure 8**A, arrowheads), but similar granules from normal RPE cells and RPE cells with AMD lacked these borders (data not shown). Melanosome-rich aceruloplasminemic RPE cells also had vesicles with granular electron-dense material (Figure 8A, arrow), but normal cells and those with AMD did not (data not shown). Analysis via SIMS demonstrated that the grainy borders on the outer edges of the complex and lipofuscin granules were iron, as was the material in the vesicles (Figure 8A [arrow], D, and E). Melanosomes contained some iron and high sulfur levels (Figure 8C-F).

The melanosome-poor cells had only siderosomes (Figure 8G) that contained very high amounts of iron, phosphorus, and sulfur (Figure 8G, J, and K). Compared with melanosome-rich cells, this iron content was much higher (Figure 8M and N).

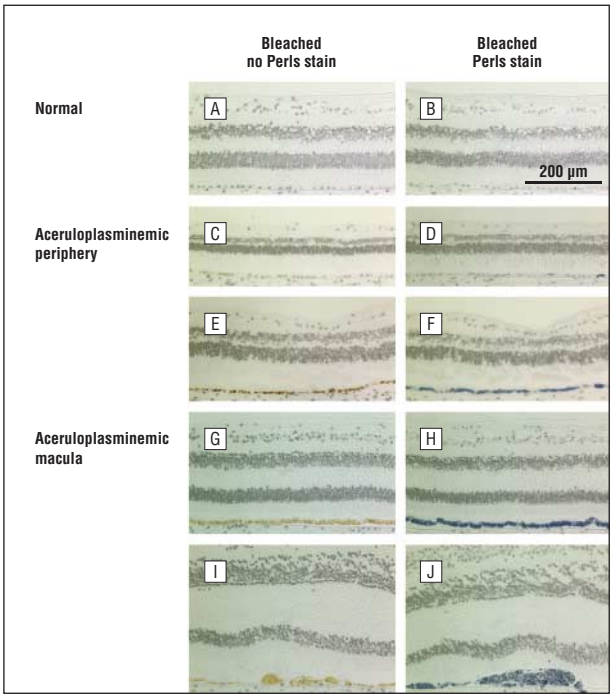

Figure 4. Macular and peripheral retina sections stained with Perls Prussian blue for iron (original magnification ×20). A, C, E, G, and I, Bleached sections not stained with Perls stain. B, D, F, H, and J, Bleached sections stained with Perls stain for iron (blue). A and B, Normal retina. C-F, Aceruloplasminemic peripheral retina. G-J, Aceruloplasminemic macular retina. J, Hypertropic retinal pigment epithelium cells.

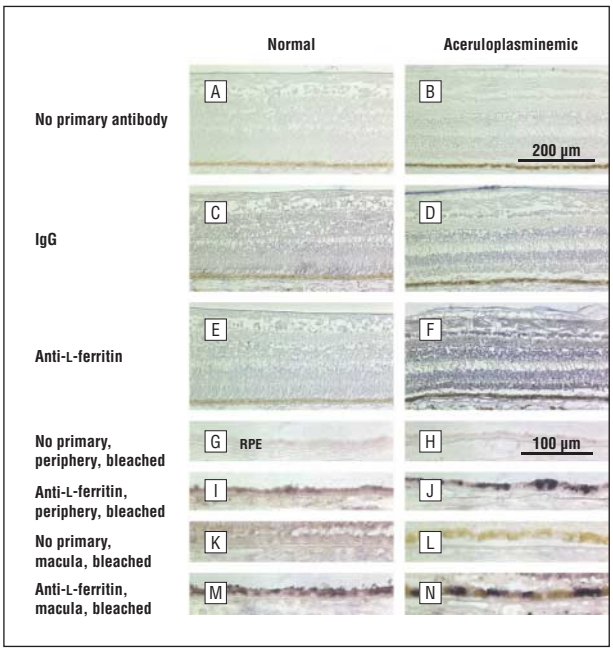

Figure 5. Normal and aceruloplasminemic retinas immunostained for L-ferritin (original magnifications: parts A-F, ×20; parts G-N, ×40). A and B, No primary antibody. C and D, IgG control staining. E and F, Anti-L-ferritin. G-N, Sections were bleached before L-ferritin stain to remove melanin. G and H, No primary antibody, peripheral retina. I and J, L-ferritin, peripheral retina. K and L, No primary antibody, macula. M and N, L-ferritin, macula.

©2011 American Medical Association. All rights reserved.
Downloaded From: https://jamanetwork.com/ on 03/04/2022

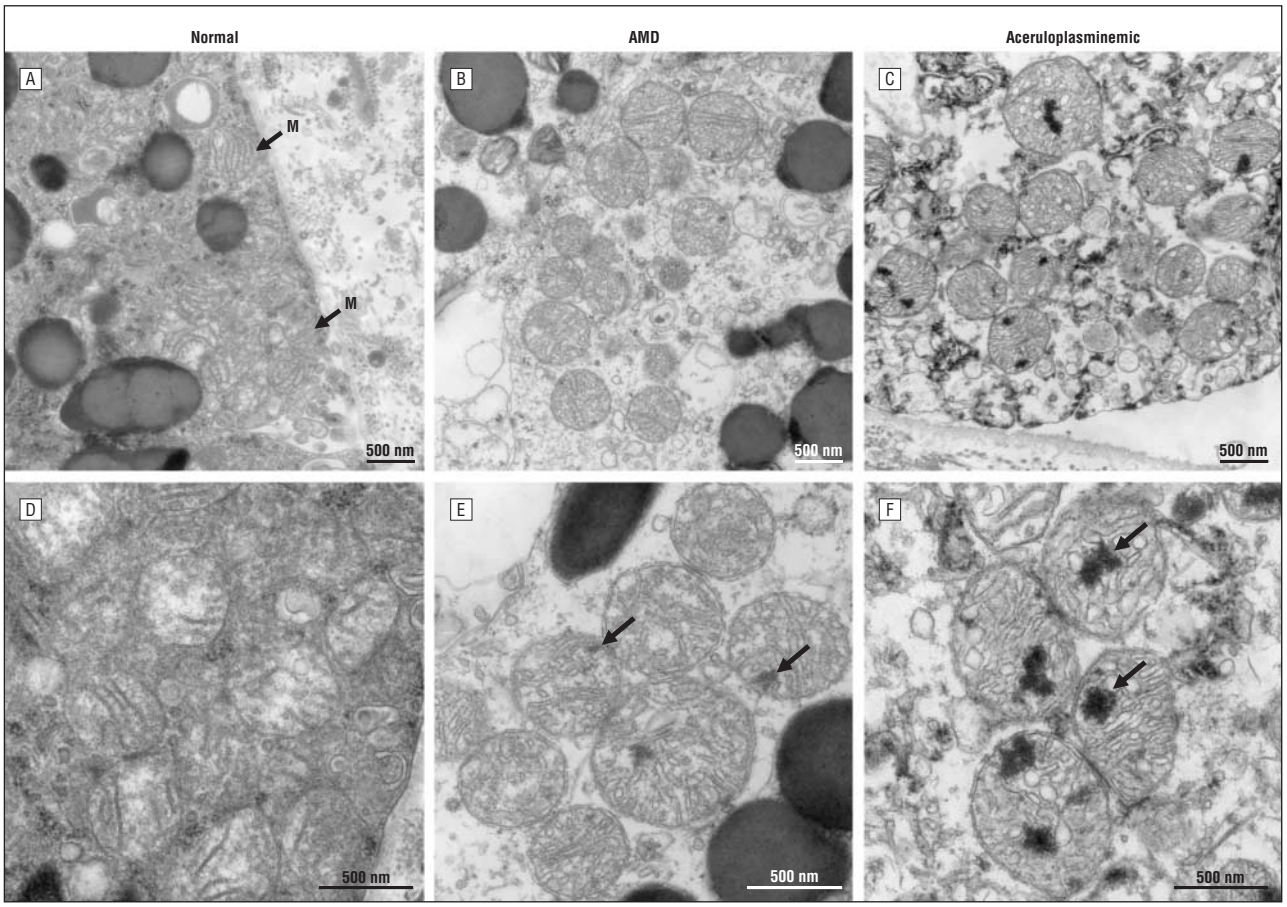

Figure 6. Mitochondria of the retinal pigment epithelium (RPE) (original magnifications: parts A-C, ×30 000; parts D-F, ×60 000). A and D, Normal RPE; B and E, RPE with age-related macular degeneration (AMD); C and F, Aceruloplasminemic RPE. Arrows indicate electron-dense inclusions; M with arrow, mitochondria.

COMMENT

We have presented for the first time, to our knowledge, the retinal histopathologic features of aceruloplasminemia and evidence for iron-mediated melanosome degradation. The aceruloplasminemic eye had many similarities to but also notable differences from eyes with AMD. Because this donor had died at age 60 years, it is possible that some of the AMD-like changes were the result of aging or AMD; however, disease was clinically evident from age 47 years, suggesting that most of our findings are the result of aceruloplasminemia.[15]

As in AMD, depigmentation, atrophy, hypertrophy, inclusions, and extrusion of the RPE were observed (Figure 1).[16] These morphologic features of these conditions were similar to those seen in AMD; however, the extent of depigmentation was greater than in AMD. Depigmented cells are found mostly in the macula in AMD, but in aceruloplasminemia they were present in the macula and in the periphery.[16]

The aceruloplasminemic eye had drusen, basal linear deposits, and deposits in the subretinal space (Figure 1 and Figure 2).[22,27] Although the morphologic findings regarding deposits were similar to AMD at the light microscopic and electron microscopic levels,[16,25,26] the distribution differed from that which is typical of AMD. The aceruloplasminemic eye had many drusen in the periphery and fewer in the macula, but the opposite is true in AMD.[16,20,35] The aceruloplasminemic eye also had a greater number of subretinal drusenoid deposits in the macula than is typical in AMD.[22]

In AMD, drusen contain activated complement. The terminal component of the complement cascade, C5b-9 (membrane attack complex), is present in most AMD nodular and diffuse drusen in a mottled pattern.[29,36] The aceruloplasminemic drusen had positive results for C5b-9 and had the expected mottled pattern; however, not all drusen were labeled (data not shown). Aceruloplasminemic diffuse drusen had more frequent C5b-9 staining than did nodular drusen, but in AMD staining is similar in both types.[36]

Vitronectin, a plasma protein that inhibits the formation of the membrane attack complex, is present in high levels in all AMD drusen[28,30] and is also seen in occasional RPE cells.[30] Similar to AMD, vitronectin strongly labeled all aceruloplasminemic drusen and occasional RPE cells (Figure 3). Subretinal drusenoid deposits had negative results for C5b-9 and vitronectin (Figure 3).

Eyes with AMD have increased iron levels in the RPE compared with normal controls, as detected by enhanced Perls stain.[10] As in AMD, aceruloplasminemic RPE cells had increased iron levels; however, the levels were so high that they could be detected by unenhanced Perls stain in all sections (Figure 4). Some aceruloplasmin-

©2011 American Medical Association. All rights reserved.
Downloaded From: https://jamanetwork.com/ on 03/04/2022

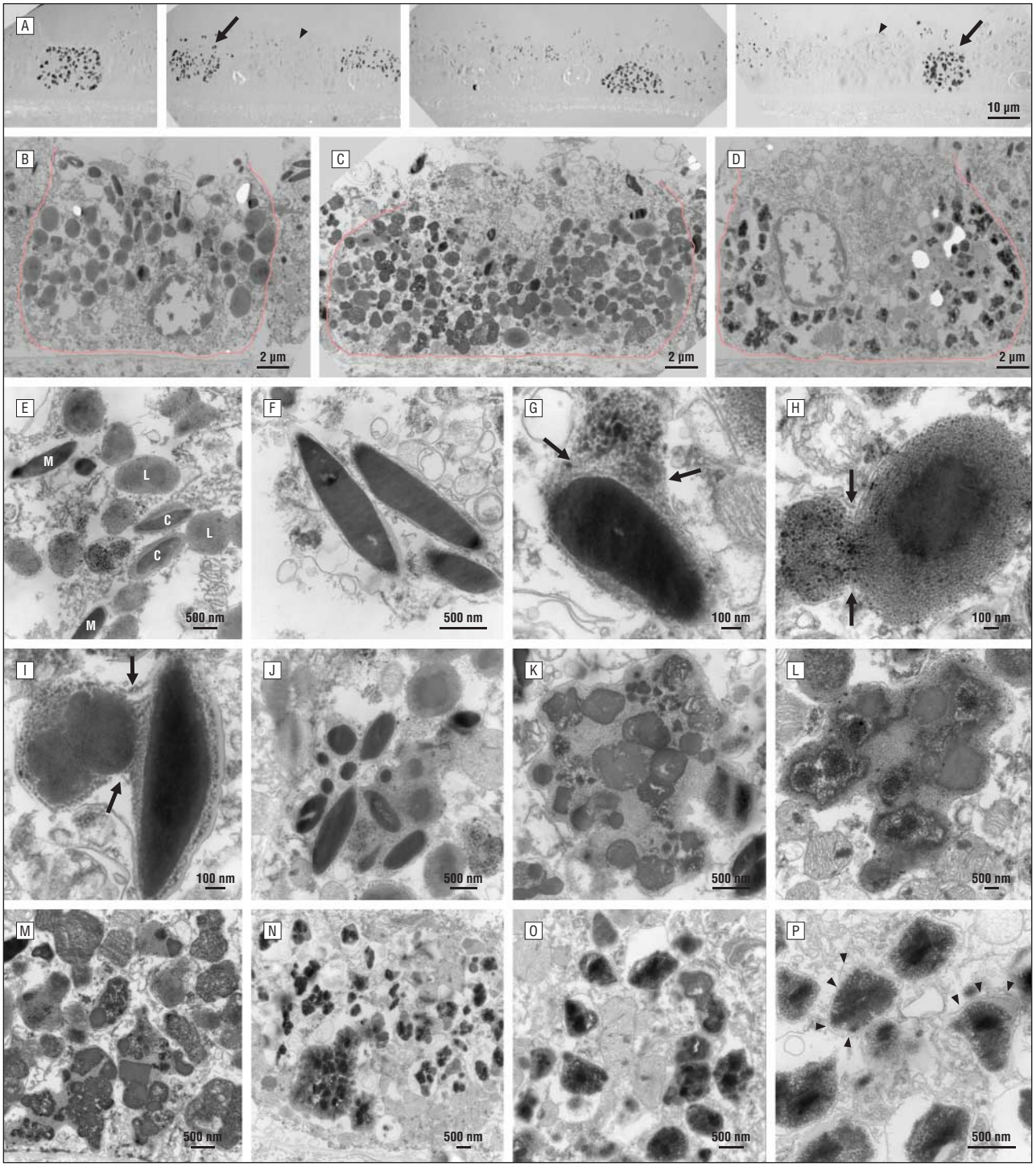

Figure 7. Granules and melanosome degradation in retinal pigment epithelium (RPE) (original magnifications: part A, ×2500; parts B-D, ×6000; parts E, M, and O, ×25 000; parts F and P, ×50 000; parts G and I, ×100 000; part H, ×75 000; part J, ×30 000; parts K and L, ×40 000; and part N, ×15 000). A, Melanosome-rich (arrowhead) and melanosome-poor (arrow) RPE cells on unstained sections by electron microscopy (EM). B, Melanosome-rich cell on stained EM. C, Intermediate cell on stained EM. D, A melanosome-poor cell on stained EM. E, Melanosomes (M), lipofuscin (L), and complex granules (C) in a melanosome-rich RPE cell. F, Normal melanosomes in a melanosome-rich RPE cell. G, Melanosome fusing (arrows) with lipofuscin or lysosomal granule in melanosome-rich RPE cell. H, Complex granule fusing (arrows) with additional lipofuscin granule. I, Two complex granules fusing (arrows) in a melanosome-rich cell. J, Aggregate of intact melanosomes and lipofuscinoid material in a melanosome-rich cell. K and L, Aggregate of melanosomes and lipofuscinoid material, with degrading melanosomes in a melanosome-rich cell. M, Aggregates of degraded melanosomes and lipofuscinoid material in an intermediate RPE cell. N, Irregular electron-dense granules in a melanosome-poor RPE cell; some granules are aggregated, others are dispersed. O and P, Irregular electron-dense granules in a melanosome-poor RPE cell; arrowheads indicate limiting membranes.

emic RPE cells, especially in the macula, had so much iron that it was visible as a golden color that could not be bleached out (Figure 4). The aceruloplasminemic macula had more iron than the periphery (Figure 4); the same was true of the normal retina (Figure 5), suggesting that RPE cells of the macula and the periphery handle

©2011 American Medical Association. All rights reserved.
Downloaded From: https://jamanetwork.com/ on 03/04/2022

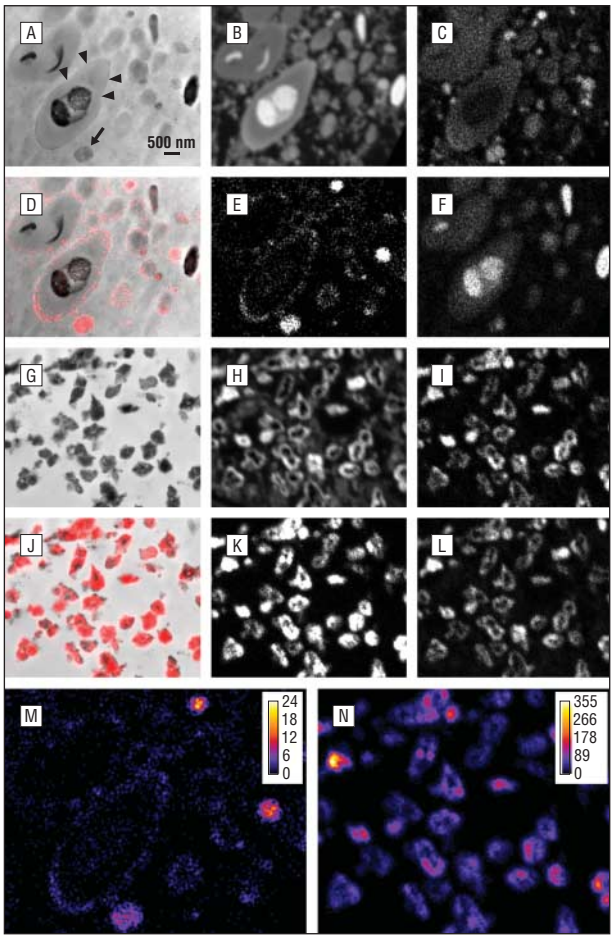

Figure 8. Secondary ion mass spectrometry (SIMS) analysis on melanosome-rich and melanosome-poor retinal pigment epithelial cells (original magnification ×20 000). A-F, Melanosome-rich cell. A, Electron microscopic results for an unstained section. Arrow indicates vesicle with electron-dense granular material (containing iron). Arrowheads indicate electron-dense granular rim (containing iron) on a complex granule. B-F, NanoSIMS analysis of the same section. B, Carbon-nitrogen. C, Phosphorus. D, Iron-oxygen map (red) overlaid onto the image on electron microscopy (EM). E, Iron-oxygen. F, Sulfur. G-L, Melanosome-poor cell. G, Unstained section by EM. H-L, NanoSIMS analysis of the same section. H, Carbon-nitrogen. I, Phosphorus. J, Iron-oxygen map (red) overlaid onto the EM image. K, Iron-oxygen. L, Sulfur. M-N, Iron-oxygen gradient map comparing iron levels in melanosome-rich (M) and melanosome-poor (N) cells.

iron in different ways[37] or that the RPE in different regions may be exposed to different iron levels. Whether similar regional differences exist in AMD has not been shown.[10]

Because the aceruloplasminemic neural retina and some RPE cells did not stain with Perls stain, we used L-ferritin immunostaining as a more sensitive test for elevated iron levels. Because ceruloplasmin is normally expressed by several retinal cell types, including Muller cells and retinal astrocytes, increased iron levels in the aceruloplasminemic neural retina were expected.[38-40] Indeed, L-ferritin levels in the aceruloplasminemic retina were elevated (Figure 5). Also, aceruloplasminemic RPE cells from the periphery and the macula had greater L-ferritin levels than normal RPE (Figure 5). Of interest, the golden, iron-laden RPE cells did not stain strongly for L-ferritin. Rather, neighboring cells that lacked the golden deposits had high levels of L-ferritin (Figure 5), suggesting that iron in the aceruloplasminemic RPE cells may be present in 2 forms, ferritin and hemosiderin.

As cells accumulate iron, they first store it in ferritin. Once the ferritin system becomes overwhelmed, iron is stored as hemosiderin in siderosomes.[33,41] Hemosiderin is a large, irregularly shaped, insoluble, crystalline aggregate of iron and other minerals; the iron comes from the cores of degraded ferritin molecules.[33,42] Immunoelectron microscopic studies[43] have demonstrated that the ferritin label in siderosomes is weak because ferritin is degraded. In the aceruloplasminemic eye, the irregularly shaped granules resembled siderosomes (Figure 7 and Figure 8),[34,44,45] which explains why the iron-laden golden RPE had lower-than-expected levels of ferritin. The difference in macular and peripheral subcellular iron distribution in the RPE may help explain the discrepancy in drusen distribution in aceruloplasminemic eyes and those with AMD. Iron distribution in maculas with AMD is more similar to that in the aceruloplasminemic periphery than in the aceruloplasminemic macula. Thus, the aceruloplasminemic periphery may better represent iron loading in AMD.

Aceruloplasminemic RPE cells had mitochondrial pathology (Figure 6). Most aceruloplasminemic mitochondria had at least 1 large focus of electron-dense material that was not iron but was likely damaged lipid and protein. The eye with AMD, which had a longer postmortem interval than the aceruloplasminemic eye, had only occasional mitochondrial accumulations, which were much smaller than those in aceruloplasminemia. The presence of mitochondrial damage in aceruloplasminemia supports previous biochemical studies[46-48] of aceruloplasminemic brains, which demonstrated mitochondrial dysfunction of respiratory chain complexes I and IV.

Melanosomes, lipofuscin, and complex granules of aceruloplasminemic RPE cells also differed from RPE cells with AMD and normal RPE cells (Figure 7 and Figure 8).[32] A typical macular RPE cell from a normal 60-year-old eye has 17 to 20 lipofuscin, 11 to 13 melanin, and 9 to 14 complex granules per cell profile.[17] The aceruloplasminemic RPE macular cells contained 2 types of cells, melanosome rich and melanosome poor, both with abnormal numbers of granules. Melanosome-rich RPE cells had greater-than-expected numbers of lipofuscin granules and melanosomes per cell profile (35 and 20, respectively) but normal numbers of complex granules. The melanosome-poor cells, however, had significantly lower numbers of each granule type (approximately 1 of each per cell profile), suggesting that the melanosomes may have been degraded.

Melanosome degradation in the RPE is controversial,[49] mainly because limited in vivo evidence has been published.[49-51] Melanosome degradation has been described in fetal bovine RPE cells as the tapetum lucidum becomes amelanotic.[50,51] As presented by Feeney-Burns and Mixon,[50] the melanosomes in the tapetal RPE form aggregates of degrading melanosomes similar to the aggregates of degrading melanosomes that we observed in the aceruloplasminemic RPE (Figure 7). The mechanism of melanosome degradation in the tapetal RPE is not clear. Feeney-Burns and Mixon, along with the au-

©2011 American Medical Association. All rights reserved.
Downloaded From: https://jamanetwork.com/ on 03/04/2022

thors of some contemporaneous studies,[32,52,53] suggest that the presence of lysosomal enzymes in melanosomes implies melanosome degradation by lysosomes. However, it is now known that melanosomes are lysosome-related organelles that normally contain lysosomal enzymes and cannot be degraded easily.[49,54,55]

Melanosomes can, however, be photodegraded[56,57] and degraded with hydrogen peroxide.[49,58] Moreover, in vitro experiments have shown that the rate of synthetic melanin degradation is significantly increased when iron or copper is added to the reaction.[58] Abundant iron in the melanosomes, lipofuscin, and complex granules of the aceruloplasminemic RPE (Figure 7 and Figure 8) suggests that melanosomes may disappear from RPE because of iron-mediated degradation. Melanosomes in melanosome-rich RPE contain very high levels of sulfur (Figure 8), whereas melanosome-poor RPE cells have high sulfur levels in the siderosomes, suggesting that components of degraded melanosomes are present in the hemosiderin. Thus, the aceruloplasminemic RPE cells may be an in vivo example of what has been observed in vitro. In conclusion, our studies have shown that RPE cells are greatly affected by the loss of ceruloplasmin; they accumulate iron and develop an AMD-like condition with many unique features.

Submitted for Publication: April 11, 2011; final revision received June 22, 2011; accepted June 28, 2011.
Correspondence: Joshua L. Dunaief, MD, PhD, F. M. Kirby Center for Molecular Ophthalmology, Scheie Eye Institute, Perelman School of Medicine, University of Pennsylvania, 305 Stellar Chance Labs, 422 Curie Blvd, Philadelphia, PA 19104 (jdunaief@mail.med.upenn.edu).
Financial Disclosure: None reported.
Funding/Support: This study was supported by National Institutes of Health grants R01EY015240, EY012211, EY012261, and EY012279 (Dr Dunaief) and 1F30AG037289-01 (Dr Wolkow), an unrestricted grant from Research to Prevent Blindness, the F. M. Kirby Foundation, a gift from L. Stanley Mauger, JD, in memory of Lee F. Mauger, MD, and the Paul and Evanina Bell Mackall Foundation Trust.
Additional Contributions: The Platform for Cell and Tissue Imaging (PICT-IBiSA) imaging facility in the Institut Curie and Raymond P. Meade, MS, at the University of Pennsylvania Electron Microscopy Resource Laboratory provided outstanding technical assistance.

REFERENCES

1. Miyajima H, Kohno S, Takahashi Y, Yonekawa O, Kanno T. Estimation of the gene frequency of aceruloplasminemia in Japan. *Neurology*. 1999;53(3):617-619.
2. Yoshida K, Furihata K, Takeda S, et al. A mutation in the ceruloplasmin gene is associated with systemic hemosiderosis in humans. *Nat Genet*. 1995;9(3):267-272.
3. Miyajima H, Nishimura Y, Mizoguchi K, Sakamoto M, Shimizu T, Honda N. Familial apoceruloplasmin deficiency associated with blepharospasm and retinal degeneration. *Neurology*. 1987;37(5):761-767.
4. Morita H, Ikeda S, Yamamoto K, et al. Hereditary ceruloplasmin deficiency with hemosiderosis: a clinicopathological study of a Japanese family. *Ann Neurol*. 1995;37(5):646-656.
5. Miyajima H. Aceruloplasminemia, an iron metabolic disorder. *Neuropathology*. 2003;23(4):345-350.
6. Harris ZL, Durley AP, Man TK, Gitlin JD. Targeted gene disruption reveals an essential role for ceruloplasmin in cellular iron efflux. *Proc Natl Acad Sci U S A*. 1999;96(19):10812-10817.
7. Patel BN, David S. A novel glycosylphosphatidylinositol-anchored form of ceruloplasmin is expressed by mammalian astrocytes. *J Biol Chem*. 1997;272(32):20185-20190.
8. De Domenico I, Ward DM, di Patti MCB, et al. Ferroxidase activity is required for the stability of cell surface ferroportin in cells expressing GPI-ceruloplasmin. *EMBO J*. 2007;26(12):2823-2831.
9. McKie AT, Marciani P, Rolfs A, et al. A novel duodenal iron-regulated transporter, IREG1, implicated in the basolateral transfer of iron to the circulation. *Mol Cell*. 2000;5(2):299-309.
10. Hahn P, Milam AH, Dunaief JL. Maculas affected by age-related macular degeneration contain increased chelatable iron in the retinal pigment epithelium and Bruch's membrane. *Arch Ophthalmol*. 2003;121(8):1099-1105.
11. Chowers I, Wong R, Dentchev T, et al. The iron carrier transferrin is upregulated in retinas from patients with age-related macular degeneration. *Invest Ophthalmol Vis Sci*. 2006;47(5):2135-2140.
12. Hahn P, Qian Y, Dentchev T, et al. Disruption of ceruloplasmin and hephaestin in mice causes retinal iron overload and retinal degeneration with features of age-related macular degeneration. *Proc Natl Acad Sci U S A*. 2004;101(38):13850-13855.
13. Hadziahmetovic M, Dentchev T, Song Y, et al. Ceruloplasmin/hephaestin knockout mice model morphologic and molecular features of AMD. *Invest Ophthalmol Vis Sci*. 2008;49(6):2728-2736.
14. Yamaguchi K, Takahashi S, Kawanami T, Kato T, Sasaki H. Retinal degeneration in hereditary ceruloplasmin deficiency. *Ophthalmologica*. 1998;212(1):11-14.
15. Dunaief JL, Richa C, Franks EP, et al. Macular degeneration in a patient with aceruloplasminemia, a disease associated with retinal iron overload. *Ophthalmology*. 2005;112(6):1062-1065.
16. Bressler NM, Silva JC, Bressler SB, Fine SL, Green WR. Clinicopathologic correlation of drusen and retinal pigment epithelial abnormalities in age-related macular degeneration. *Retina*. 1994;14(2):130-142.
17. Feeney-Burns L, Hilderbrand ES, Eldridge S. Aging human RPE: morphometric analysis of macular, equatorial, and peripheral cells. *Invest Ophthalmol Vis Sci*. 1984;25(2):195-200.
18. Guerquin-Kern J-L, Wu T-D, Quintana C, Croisy A. Progress in analytical imaging of the cell by dynamic secondary ion mass spectrometry (SIMS microscopy). *Biochim Biophys Acta*. 2005;1724(3):228-238.
19. Green WR, McDonnell PJ, Yeo JH. Pathologic features of senile macular degeneration. *Ophthalmology*. 1985;92(5):615-627.
20. Spraul CW, Grossniklaus HE. Characteristics of drusen and Bruch's membrane in postmortem eyes with age-related macular degeneration. *Arch Ophthalmol*. 1997;115(2):267-273.
21. Sarks SH, Arnold JJ, Killingsworth MC, Sarks JP. Early drusen formation in the normal and aging eye and their relation to age related maculopathy: a clinicopathological study. *Br J Ophthalmol*. 1999;83(3):358-368.
22. Rudolf M, Malek G, Messinger JD, Clark ME, Wang L, Curcio CA. Sub-retinal drusenoid deposits in human retina: organization and composition. *Exp Eye Res*. 2008;87(5):402-408.
23. Sarks JP, Sarks SH, Killingsworth MC. Evolution of soft drusen in age-related macular degeneration. *Eye (Lond)*. 1994;8(pt 3):269-283.
24. Sarks SH. Ageing and degeneration in the macular region: a clinico-pathological study. *Br J Ophthalmol*. 1976;60(5):324-341.
25. Burns RP, Feeney-Burns L. Clinico-morphologic correlations of drusen of Bruch's membrane. *Trans Am Ophthalmol Soc*. 1980;78:206-225.
26. Feeney-Burns L, Ellersieck MR. Age-related changes in the ultrastructure of Bruch's membrane. *Am J Ophthalmol*. 1985;100(5):686-697.
27. Hogan MJ, Alvarado JA, Weddell JE. *Histology of the Human Eye: An Atlas and Textbook*. Philadelphia, PA: WB Saunders Co; 1971.
28. Hageman GS, Mullins RF, Russell SR, Johnson LV, Anderson DH. Vitronectin is a constituent of ocular drusen and the vitronectin gene is expressed in human retinal pigmented epithelial cells. *FASEB J*. 1999;13(3):477-484.
29. Johnson LV, Ozaki S, Staples MK, Erickson PA, Anderson DH. A potential role for immune complex pathogenesis in drusen formation. *Exp Eye Res*. 2000;70(4):441-449.
30. Johnson LV, Leitner WP, Staples MK, Anderson DH. Complement activation and inflammatory processes in drusen formation and age related macular degeneration. *Exp Eye Res*. 2001;73(6):887-896.
31. Anderson DH, Radeke MJ, Gallo NB, et al. The pivotal role of the complement system in aging and age-related macular degeneration: hypothesis re-visited. *Prog Retin Eye Res*. 2010;29(2):95-112.
32. Feeney L. Lipofuscin and melanin of human retinal pigment epithelium: fluorescence, enzyme cytochemical, and ultrastructural studies. *Invest Ophthalmol Vis Sci*. 1978;17(7):583-600.
33. Wixom RL, Prutkin L, Munro HN. Hemosiderin: nature, formation, and significance. *Int Rev Exp Pathol*. 1980;22:193-225.

©2011 American Medical Association. All rights reserved.
Downloaded From: https://jamanetwork.com/ on 03/04/2022

34. Richter GW. Studies of iron overload: rat liver siderosome ferritin. *Lab Invest*. 1984;50(1):26-35.
35. Abdelsalam A, Del Priore L, Zarbin MA. Drusen in age-related macular degeneration: pathogenesis, natural course, and laser photocoagulation-induced regression. *Surv Ophthalmol*. 1999;44(1):1-29.
36. Mullins RF, Russell SR, Anderson DH, Hageman GS. Drusen associated with aging and age-related macular degeneration contain proteins common to extracellular deposits associated with atherosclerosis, elastosis, amyloidosis, and dense deposit disease. *FASEB J*. 2000;14(7):835-846.
37. Burke JM, Hjelmeland LM. Mosaicism of the retinal pigment epithelium: seeing the small picture. *Mol Interv*. 2005;5(4):241-249.
38. Klomp LWJ, Farhangrazi ZS, Dugan LL, Gitlin JD. Ceruloplasmin gene expression in the murine central nervous system. *J Clin Invest*. 1996;98(1):207-215.
39. Klomp LWJ, Gitlin JD. Expression of the ceruloplasmin gene in the human retina and brain: implications for a pathogenic model in aceruloplasminemia. *Hum Mol Genet*. 1996;5(12):1989-1996.
40. Levin LA, Geszvain KM. Expression of ceruloplasmin in the retina: induction after optic nerve crush. *Invest Ophthalmol Vis Sci*. 1998;39(1):157-163.
41. Harrison PM, Arosio P. The ferritins: molecular properties, iron storage function and cellular regulation. *Biochim Biophys Acta*. 1996;1275(3):161-203.
42. Koorts AM, Viljoen M. Ferritin and ferritin isoforms I: structure-function relationships, synthesis, degradation and secretion. *Arch Physiol Biochem*. 2007; 113(1):30-54.
43. Cooper PJ, Iancu TC, Ward RJ, Guttridge KM, Peters TJ. Quantitative analysis of immunogold labelling for ferritin in liver from control and iron-overloaded rats. *Histochem J*. 1988;20(9):499-509.
44. Richter GW. Electron microscopy of hemosiderin; presence of ferritin and occurrence of crystalline lattices in hemosiderin deposits. *J Biophys Biochem Cytol*. 1958;4(1):55-58.
45. Iancu TC. Ferritin and hemosiderin in pathological tissues. *Electron Microsc Rev*. 1992;5(2):209-229.
46. Yoshida K, Kaneko K, Miyajima H, et al. Increased lipid peroxidation in the brains of aceruloplasminemia patients. *J Neurol Sci*. 2000;175(2):91-95.
47. Miyajima H, Kono S, Takahashi Y, Sugimoto M. Increased lipid peroxidation and mitochondrial dysfunction in aceruloplasminemia brains. *Blood Cells Mol Dis*. 2002;29(3):433-438.
48. Kohno S, Miyajima H, Takahashi Y, Suzuki H, Hishida A. Defective electron transfer in complexes I and IV in patients with aceruloplasminemia. *J Neurol Sci*. 2000; 182(1):57-60.
49. Borovanský J, Elleder M. Melanosome degradation: fact or fiction. *Pigment Cell Res*. 2003;16(3):280-286.
50. Feeney-Burns L, Mixon RN. Development of amelanotic retinal pigment epithelium in eyes with a tapetum lacidum: melanosome autophagy and termination of melanogenesis. *Dev Biol*. 1979;72(1):73-88.
51. Garcia RI, Flynn EA, Szabo G. Autophagocytosis of melanosomes in cultured embryonic retinal pigment cells. *Experientia*. 1983;39(4):391-392.
52. Feeney-Burns L, Gao C-L, Tidwell M. Lysosomal enzyme cytochemistry of human RPE, Bruch's membrane and drusen. *Invest Ophthalmol Vis Sci*. 1987; 28(7):1138-1147.
53. Kim IT, Choi JB. Melanosomes of retinal pigment epithelium—distribution, shape, and acid phosphatase activity. *Korean J Ophthalmol*. 1998;12(2):85-91.
54. Raposo G, Marks MS. Melanosomes—dark organelles enlighten endosomal membrane transport. *Nat Rev Mol Cell Biol*. 2007;8(10):786-797.
55. Bhatnagar V, Anjaiah S, Puri N, Darshanam BNA, Ramaiah A. pH of melanosomes of B 16 murine melanoma is acidic: its physiological importance in the regulation of melanin biosynthesis. *Arch Biochem Biophys*. 1993;307(1):183-192.
56. Zareba M, Szewczyk G, Sarna T, et al. Effects of photodegradation on the physical and antioxidant properties of melanosomes isolated from retinal pigment epithelium. *Photochem Photobiol*. 2006;82(4):1024-1029.
57. Sarna T, Burke JM, Korytowski W, et al. Loss of melanin from human RPE with aging: possible role of melanin photooxidation. *Exp Eye Res*. 2003;76(1):89-98.
58. Korytowski W, Sarna T. Bleaching of melanin pigments: role of copper ions and hydrogen peroxide in autooxidation and photooxidation of synthetic dopa-melanin. *J Biol Chem*. 1990;265(21):12410-12416.

Visit www.archophthalmol.com. As an individual subscriber you can use the Citation Manager. You can download article citations in the Medlars format compatible with import into personal bibliographic management software such as EndNote, Reference Manager, or ProCite.

©2011 American Medical Association. All rights reserved.
Downloaded From: https://jamanetwork.com/ on 03/04/2022